

# Mapping of vibrational wave-packet motion by femtosecond time-resolved kinetic energy time-of-flight mass spectroscopy

A. Assion<sup>1</sup>, T. Baumert<sup>2</sup>, M. Geisler<sup>1</sup>, V. Seyfried<sup>1</sup>, and G. Gerber<sup>1,a</sup>

<sup>1</sup> Physikalisches Institut, Universität Würzburg, Am Hubland, 97074 Würzburg, Germany

<sup>2</sup> Deutsches Zentrum für Luft-und Raumfahrt, Oberpfaffenhofen, 82230 Weßling, Germany

Received: 16 March 1998 / Received in final form and Accepted: 2 June 1998

**Abstract.** Kinetic energy time-of-flight (KETOF) mass spectroscopy in combination with femtosecond pump-probe and molecular beam techniques is used to map molecular dynamics along an internuclear coordinate. By recording transient KETOF mass spectra we monitor the vibrational wave-packet motion on a neutral electronic state for all possible internuclear distances simultaneously. The power of this method is demonstrated by the one dimensional wave-packet motion on the  $2^1\Sigma_u^+$  double minimum state of the sodium dimer. For comparison with the experiment quantum mechanical simulations were performed.

**PACS.** 33.80.-b Photon interactions with molecules – 39.30.+w Spectroscopic techniques – 31.70.Hq Time-dependent phenomena: excitation and relaxation processes, and reaction rates – 82.50.Fv Photolysis, photodissociation, and photoionization by infrared, visible, and ultraviolet radiation

In recent years femtosecond laser spectroscopy has become a standard tool for time-resolved studies of molecular processes (for a review on this topic see for example [1,2] and references therein). Pump-probe-experiments have opened up the opportunity to study molecular dynamics in real time. However, the real-time observation of structural changes in a molecule is still a challenging task. Approaches using ultrafast electron diffraction [3] or ultrafast X-ray diffraction [4,5] are experimentally rather demanding. On the other hand standard pump-probe techniques using for example detection of laser-induced fluorescence [6,7], ionization mass spectroscopy [8,9] or zero kinetic energy electron (ZEKE) spectroscopy [10,11] limit the observation of molecular dynamics to a small range of internuclear distances. This is because narrow Franck-Condon windows for electronic transitions have to be used in order to assign the detected signal to the corresponding internuclear distance. If there is, however, an additional experimental parameter directly corresponding to the internuclear distance of laser induced transitions, the detection of nuclear motion is feasible over a wide range of internuclear distances. Such a desired parameter is for instance the energy of the photoelectrons released in a molecular ionization process as proposed by Seel and Domcke [12] and applied to Na<sub>2</sub> by Meier and Engel [13]. This correspondence has been demonstrated in a recent publication [14], where femtosecond pump-probe photoelectron spectroscopy was employed to map the molecular wave-packet motion in the  $2^1\Pi_g$  state of the sodium dimer over the whole range of possible internuclear distances.

Extensions of this technique to polyatomic molecules have recently been reported [15–17]. Besides the photoelectron energy also the kinetic energy of the fragments generated in molecular dissociation processes can serve to determine the internuclear distance of laser induced transitions. The basic idea is, that in a direct photoionization process onto a repulsive state the kinetic energy of a fragment corresponds to a specific internuclear distance. Therefore it is possible to map the vibrational wave-packet motion over the whole range of possible internuclear distances by measuring the dependence of the fragment ion energy distribution on the delay-time between the two laser pulses in a pump-probe-experiment. This technique has already been used in the Coulomb explosion experiments by Stapelfeldt *et al.* [18], in which strong laser fields are employed to produce doubly charged ions. In contrast to this experiment we use as dissociative molecular states low-lying singly-charged repulsive ionic states. In general using low-lying ionic states for detection has several advantages. These states are accessible in relatively weak laser fields and at small internuclear distances. Additionally they are stable and unperturbed and their potential curves are often well-known. Furthermore charged particles are detected very efficiently and there are relaxed selection rules for ionizing (bound-free) transitions compared to bound-bound transitions [19,20]. The kinetic energy of the ionic fragments in our experiment is determined by kinetic energy time-of-flight mass spectroscopy (KETOF) [21], which has the additional advantage of mass-selectivity. This technique was first employed in combination with fs single-pulse excitation to study the different ionization mechanisms

<sup>a</sup> e-mail: gerber@physik.uni-wuerzburg.de

in resonance enhanced multiphoton ionization (REMPI) of the sodium dimer [22]. Pump-probe experiments in combination with the KETOF technique were initially used to detect different pathways of dissociation in IHgI [23].

The experimental setup is described in detail in reference [24] and will only be outlined briefly here. We used a home-built Ti:sapphire oscillator combined with a modified commercial regenerative amplifier to generate 90 fs, 800  $\mu\text{J}$  pulses at a wavelength of 790 nm with a repetition rate of 1 kHz. These pulses were frequency converted into pulses at 683 nm by an optical parametric generator and decompressed to 60 fs by a prism compressor. In a Michelson type setup the laser beam was split into two equal parts with a variable time delay between the two laser pulses. Then the 60 fs laser pulses were frequency doubled with a 100  $\mu\text{m}$  BBO crystal to obtain laser pulses of 341.5 nm wavelength. In order to avoid strong field effects [25,26] we attenuated the pump and probe laser pulses properly. The experiments were performed on  $\text{Na}_2$  which was produced vibrationally cold in its electronic  $X^1\Sigma_g^+$  ground state by supersonic beam expansion of pure sodium. A linear time-of-flight (TOF) spectrometer was used for ion detection.

In our experiment we map the molecular vibrational wave-packet dynamics in the  $2^1\Sigma_u^+$  double minimum state of  $\text{Na}_2$ . We have chosen this state as intermediate state in our KETOF pump-probe experiment because the intrinsic potential barrier of the  $2^1\Sigma_u^+$  state influences the wave-packet motion. The  $2^1\Sigma_u^+$  state of  $\text{Na}_2$  was theoretically predicted by Valance and Tuan [27] and was experimentally confirmed by Cooper *et al.* [28]. Further investigations with ns laser REMPI techniques by Delacrétaz and Wöste [29] and by Haugstätter *et al.* [30] followed. In a previous fs time-resolved study of vibrational wave-packet motion on this state we demonstrated that high resolution frequency spectroscopy with spectrally broad fs laser sources can be performed [31]. A theoretical publication concerning the mapping of a vibrational wave-packet propagating in this state by photoelectron spectroscopy has appeared recently [32].

The excitation scheme given in Figure 1 shows that the transition onto the repulsive ionic  $2^2\Sigma_u^+(\text{Na}_2^+)$  state of the sodium dimer ion requires two photons at a wavelength of 341.5 nm with the  $2^1\Sigma_u^+$  double minimum state as resonant intermediate state. By absorption of a first pump photon a wave-packet will be generated at the inner turning point in the  $2^1\Sigma_u^+$  double minimum state due to coherent superposition of a number of vibrational eigenstates ( $v' = 36$  to  $v' = 41$  for a 60 fs pulse at 341.5 nm). Except at very small internuclear distances a transition onto the repulsive ionic  $2^2\Sigma_u^+(\text{Na}_2^+)$  state is possible by absorption of a second photon out of the time delayed probe-pulse. In such a direct photoionization process the kinetic energy of the fragment ions can be determined by a classical difference potential analysis [33,34]. A quantum mechanical description for a similar continuous wave excitation problem can be found for example in reference [35]. The difference potential  $2^2\Sigma_u^+(\text{Na}_2^+) - 2^1\Sigma_u^+(\text{Na}_2) + h\nu$  (dashed line in

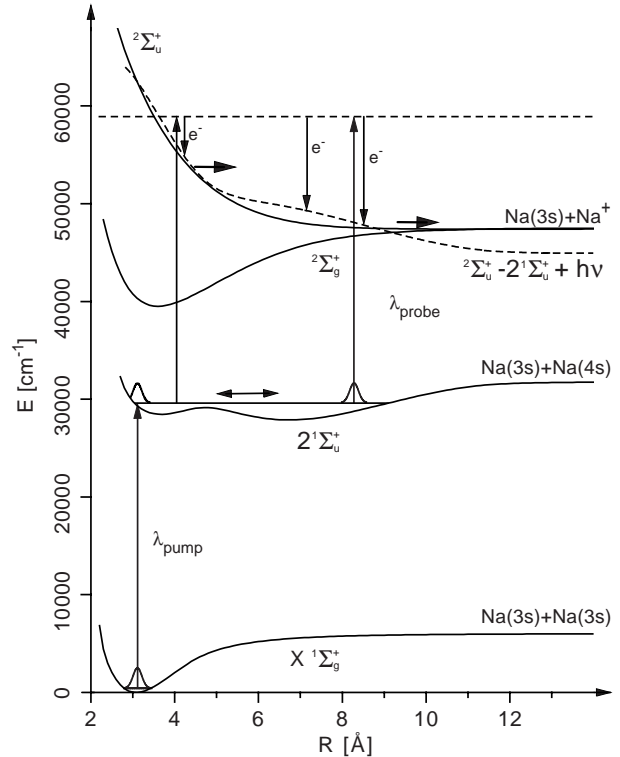


**Fig. 1.** Excitation scheme of the experiment. The pump-laser at 341.5 nm generates a vibrational wave-packet at the inner turning point of the  $2^1\Sigma_u^+$  double minimum state of the sodium dimer. The difference potential ( $2^2\Sigma_u^+(\text{Na}_2^+) - 2^1\Sigma_u^+(\text{Na}_2) + 2h\nu$ ;  $h\nu$  is the photon energy; dashed line) shows that upon direct ionization out of the  $2^1\Sigma_u^+$  double minimum state into the  $2^2\Sigma_u^+(\text{Na}_2^+)$  state the released kinetic energy of the fragment ions ( $\text{Na}^+$ ) depends on the internuclear distance. Therefore it is possible to map the vibrational wave-packet motion over the whole range of allowed internuclear distances by measuring the fragment kinetic energy distribution in a pump-probe experiment.

Fig. 1) onto which the transition proceeds shows that the released kinetic energy of the fragment ions depends on the internuclear distance where the ionization takes place and decreases with increasing internuclear distance. Therefore a direct correspondence between fragment kinetic energy and internuclear distance exists. Thus, a measurement of the dependence of the fragment kinetic energy distribution on the pump-probe delay-time maps the wave-packet evolution along the internuclear distance in real time.

Since the excitation  $X^1\Sigma_g^+ \rightarrow 2^1\Sigma_u^+$  is a  $\Sigma - \Sigma$  transition, the electronic dipole matrix element is parallel to the molecular axis. In our experiment the polarization of the laser is parallel to the TOF axis. Thus the molecules in the  $2^1\Sigma_u^+$  state are oriented with a  $\cos^2 \vartheta$  distribution along the time-of-flight axis. In energy resolved time-of-flight mass spectroscopy a fragmentation of molecules with this angular distribution leads to a typical two peak structure in the measured TOF distribution [21]. The peak at earlier TOFs belongs to ions which are produced with an initial velocity component along the direction towards the detector and the peak at larger TOFs belongs to ions

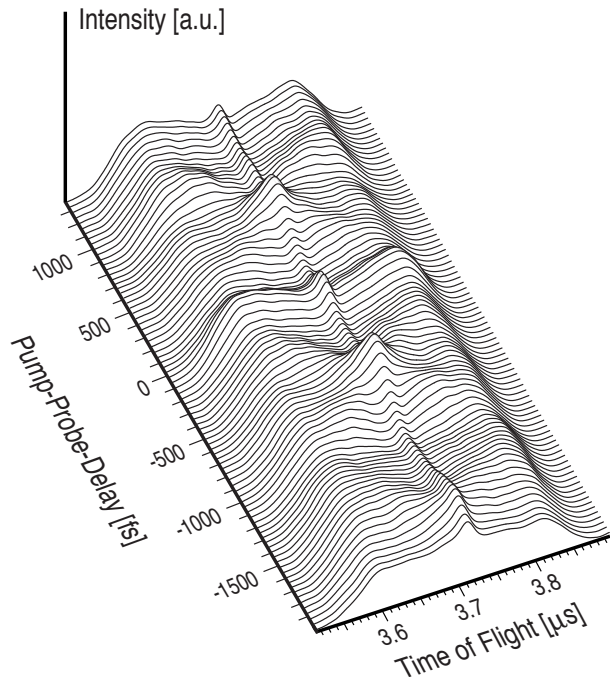


**Fig. 2.** Dependence of time-of-flight (TOF) fragment ion distributions on the pump-probe delay-time. Larger TOF differences correspond to higher fragment energies and therefore to smaller internuclear distances, whereas smaller TOF differences correspond to smaller fragment energies and therefore to larger internuclear distances. The temporal development of the wave-packet is mapped over the whole range of allowed internuclear distances.

with an initial velocity component pointing away from the detector. In our case the distribution of dissociating fragments might be modified by an anisotropy of the dipole matrix element for the ionization step. Nevertheless the maximum time-of-flight difference between the fragments ejected in direction to the detector and in the opposite direction yields quantitative information on the fragment kinetic energy. The higher the released kinetic energy the larger is the difference of time-of-flights between the two fragment peaks. In our case larger time-of-flight differences and therefore higher kinetic energies correspond to smaller internuclear distances (see Fig. 1). The experimental result is depicted in Figure 2. For each step of 20 fs in the pump-probe delay-time a total of 3000 TOF spectra was recorded and added. Additionally an averaging along the TOF axis was performed. The TOF difference between the ions ejected in direction to the detector and those ejected in the opposite direction has a maximum of  $0.34 \mu\text{s}$  which corresponds to a maximum fragment kinetic energy of  $1.35 \text{ eV}$  for the used extraction field of  $33 \text{ V/cm}$ . This is in good agreement with the value of  $1.38 \text{ eV}$  obtained from the difference potential analysis. The time-evolution of the wave-packet is beautifully resolved. The wave-packet starts at the inner turning point of the potential and moves outward, turns around, moves back in, turns again and so on. The signal decreases at small internuclear distances, *i.e.* large time-of-flight differences. This

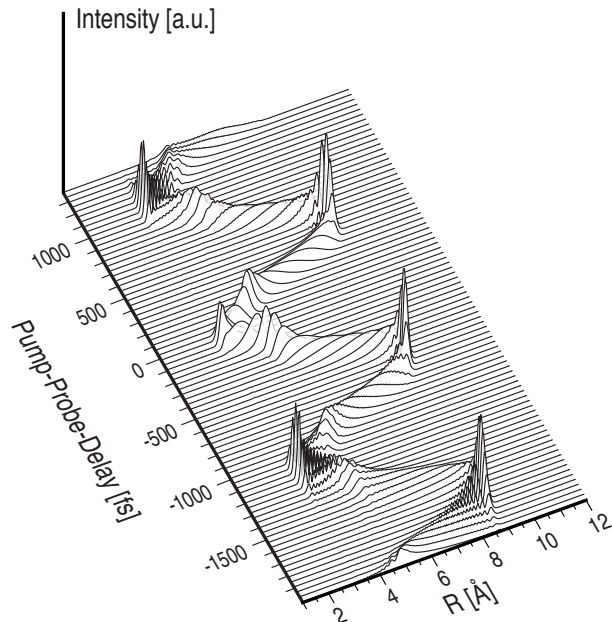


**Fig. 3.** Calculated temporal development of the wave-packet in the  $2^1\Sigma_u^+$  double minimum state of the sodium dimer. The wave-packet was generated by a 60 fs pump-pulse at  $341.5 \text{ nm}$  out of the  $X^1\Sigma_g^+$  ground state.

is due to the fact that the repulsive ionic  $2^2\Sigma_u^+$  state cannot be reached by the absorption of one photon of  $341.5 \text{ nm}$  out of the  $2^1\Sigma_u^+$  double minimum state at very small internuclear distances for energetic reasons. Note that the peak at  $3.71 \mu\text{s}$ , which corresponds to a fragment kinetic energy of  $0 \text{ eV}$ , does not originate in molecular processes but is due to REMPI ionization of atomic sodium contained in the molecular beam.

For comparison with the experiment quantum mechanical perturbation theory calculations were performed in which the temporal development was calculated with the split-operator-technique [32, 36]. In Figure 3 the calculated wave-packet dynamics in the  $2^1\Sigma_u^+$  double minimum state at a wavelength of  $341.5 \text{ nm}$  is depicted. Figure 4 shows the calculated fragment ion energy distribution. On the basis of the experimentally known spectrometer calibration (*i.e.* the relation between fragment kinetic energy and TOF) the calculated fragment ion energy distribution was transformed into TOF spectra. The result for our experimental parameters is shown in Figure 5. Note that a compression of the wave-packet at the barrier of the  $2^1\Sigma_u^+$  state occurs but it is difficult to distinguish in the TOF-spectra from contributions due to the nonlinearity of the difference potential between the  $2^2\Sigma_u^+(\text{Na}_2^+)$  state and the  $2^1\Sigma_u^+$  state. The numerical results are in good agreement with the measurement except for the minor differences discussed below. The different resolution in the simulation and the experiment is due to the fact that an averaging had to be performed on the experimental data to present them appropriately. At delay-times around  $\Delta t = 0$  when pump and probe laser pulse overlap in time, the calculation does not fully reproduce the measurement. This is

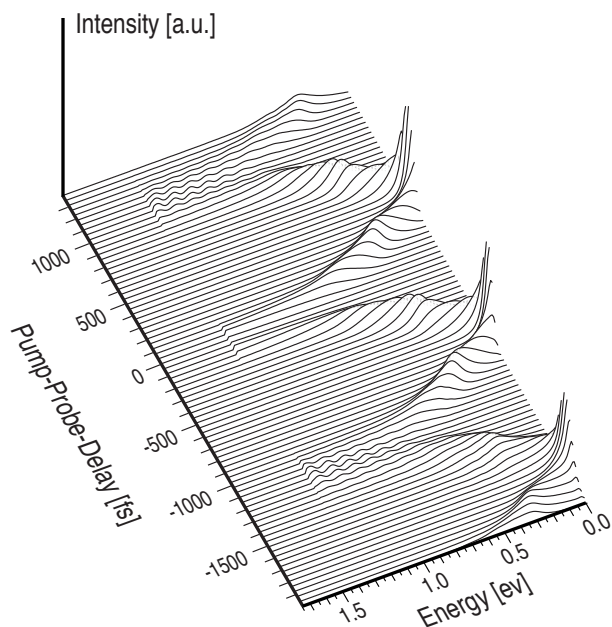


**Fig. 4.** Calculated fragment ion energy distribution for the ionization due to the interaction of a 60 fs probe-pulse at 341.5 nm with the wave-packet depicted in Figure 3.

because on the one hand in the calculation interference effects between the two laser pulses were not taken into account and on the other hand in the experimental setup the frequency doubling crystal used to produce pulses at 341.5 nm was put after the pump-probe delay-line. This leads to a higher yield of 341.5 nm light and thus to a higher ionization yield when pump and probe laser overlap temporally. Furthermore the peak at  $3.71 \mu\text{s}$ , originating in REMPI ionization of atomic sodium, can of course not be reproduced by the simulation.

In summary we have combined molecular beam kinetic energy time-of-flight mass spectroscopy with femtosecond pump-probe techniques in order to follow structural changes in a molecule upon excitation with an ultrashort laser pulse in real time along an internuclear coordinate. The one dimensional wave-packet motion on the  $2^1\Sigma_u^+$  double minimum state of the sodium dimer has been chosen to demonstrate the power of this method. The comparison of Figures 2 and 5 clearly shows that the measurement beautifully maps the propagation of the wave-packet over all internuclear distances. In contrast to conventional time-resolved photoelectron spectroscopy this method to map molecular dynamics is mass-selective. Compared to the Coulomb explosion technique, it requires a weaker laser intensity and the interaction process with the probe laser is in most cases better understood.

We would like to thank V. Engel for help and fruitful discussions. Assistance from M. Bergt and D. Woessner in handling large data files is gratefully acknowledged. We thank both referees for most valuable comments. This work was supported by the “Deutsche Forschungsgemeinschaft” and the “Fonds der chemischen Industrie”.

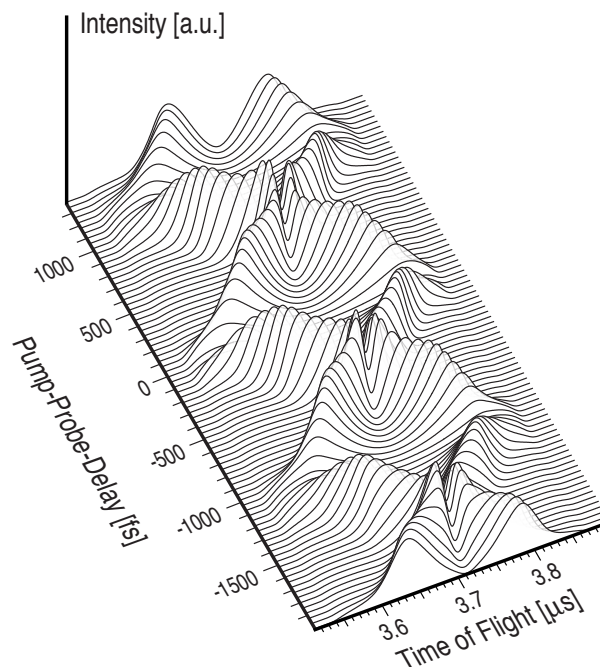


**Fig. 5.** The TOF ion spectra were calculated on the basis of the simulated fragment ion energy distribution depicted in Figure 4. The numerical results correspond very closely to the experimental results shown in Figure 2.

## References

1. *Femtochemistry: Ultrafast dynamics of the chemical bond*, edited by A.H. Zewail, Vols. 1 and 2 (World Scientific, Singapore, 1995).
2. *Femtosecond chemistry*, edited by J. Manz, L. Wöste, Vols. 1 and 2 (VCH, Weinheim, 1995).
3. J.C. Williamson, J. Cao, H. Ihee, H. Frey, A.H. Zewail, *Nature* **386**, 159 (1997).
4. M. Ben-Nun, T.J. Martínez, P.M. Weber, K.R. Wilson *Chem. Phys. Lett.* **262**, 405 (1996).
5. F.R. Rákai, K.R. Wilson, Z. Jiang, A. Ikhlef, C.Y. Côté, J.-C. Kieffer, *J. Chem. Phys.* **104**, 6066 (1996).
6. M.J. Rosker, M. Dantus, A.H. Zewail, *J. Chem. Phys.* **89**, 6113 (1988).
7. L.R. Khundkar, A.H. Zewail, *Ann. Rev. Phys. Chem.* **41**, 15 (1990).
8. T. Baumert, M. Grosser, R. Thalweiser, G. Gerber, *Phys. Rev. Lett.* **67**, 3753 (1991).
9. M. Dantus, M.H. Janssen, A.H. Zewail, *Chem. Phys. Lett.* **181**, 281 (1991).
10. T. Baumert, R. Thalweiser, G. Gerber, *Chem. Phys. Lett.* **209**, 29 (1993).
11. I. Fischer, D.M. Villeneuve, M.J.J. Vrakking, A. Stolow, *J. Chem. Phys.* **102**, 5566 (1995).
12. M. Seel, W. Domcke, *J. Chem. Phys.* **95**, 7806 (1991).
13. Ch. Meier, V. Engel, *Chem. Phys. Lett.* **212**, 691 (1993).
14. A. Assion, T. Baumert, J. Helbing, V. Seyfried, G. Gerber in *Ultrafast Phenomena X*, edited by J. Fujimoto, W. Zinth, P.F. Barbara, W.H. Knox (Springer Verlag, Berlin, Heidelberg, 1996), p. 270; A. Assion, M. Geisler, J. Helbing, V. Seyfried, T. Baumert, *Phys. Rev. A* **54**, R4605 (1996).

15. D.R. Cyr, C.C. Hayden, *J. Chem. Phys.* **104**, 771 (1995).
16. W. Radloff, V. Stert, Th. Freudenberg, I.V. Hertel, C. Jouvot, C. Dedonder-Lardeux, D. Solgadi, *Chem. Phys. Lett.* **281**, 20 (1997).
17. V. Blanchet, A. Stolow, *J. Chem. Phys.* **108**, (1998).
18. H. Stapelfeldt, E. Constant, P.B. Corkum, *Phys. Rev. Lett.* **74**, 3780 (1995).
19. S.N. Dixit, V. McKoy, *Chem. Phys. Lett.* **128**, 49 (1986).
20. J.C. Xie, R.N. Zare, *J. Chem. Phys.* **93**, 3033 (1990).
21. G.E. Hall, P.L. Houston, *Ann. Rev. Phys. Chem.* **40**, 375 (1989).
22. T. Baumert, B. Buehler, R. Thalweiser, G. Gerber, *Phys. Rev. Lett.* **64**, 733 (1990).
23. T. Baumert, S. Pedersen, A.H. Zewail, *J. Phys. Chem.* **97**, 12447 (1993).
24. T. Baumert, G. Gerber, *Adv. At. Molec. Opt. Phys.* **35**, 163 (1995).
25. *Multiphoton processes 1996*, edited by P. Lambropoulos, H. Walther (IOP Publishing, Bristol, Philadelphia, 1997).
26. T. Baumert, G. Gerber, *Physica Scripta T* **72**, 53 (1997).
27. A. Valance, Q.N. Tuan, *J. Phys. B* **15**, 17 (1982).
28. D.L. Cooper, R.F. Barrow, J. Vergés, C. Effantin, J. D'Incan, *Can. J. Phys.* **63**, 1543 (1984).
29. G. Delacrétaz, L. Wöste, *Chem. Phys. Lett.* **120**, 342 (1985).
30. R. Haugstätter, A. Goerke, I.V. Hertel, *Z. Phys. D* **9**, 153 (1988).
31. A. Assion, T. Baumert, V. Seyfried, V. Weiss, E. Wiedenmann, G. Gerber, *Z. Phys. D* **36**, 265 (1996).
32. C. Meier, V. Engel, *J. Chem. Phys.* **101**, 2673 (1994).
33. T. Baumert, B. Buehler, M. Grosser, R. Thalweiser, V. Weiss, E. Wiedenmann, G. Gerber, *J. Phys. Chem.* **95**, 8103 (1991).
34. R.S. Mulliken, *J. Chem. Phys.* **55**, 309 (1971).
35. M. Shapiro, *Chem. Phys. Lett.* **81**, 521 (1981).
36. J.A. Fleck Jr., J.R. Morris, M.D. Feit, *Appl. Phys.* **10**, 129 (1976).